



# Wave energy resource assessment with improved satellite altimetry data over the Malaysian coastal sea

Nurul Hazrina Idris<sup>1,2</sup>

Received: 13 December 2018 / Accepted: 18 July 2019 / Published online: 31 July 2019  
© Saudi Society for Geosciences 2019

## Abstract

This paper presents the assessment of wave energy resources over Malaysian seas using the improved satellite altimetry data. Instead of the standard altimetry data, the coastal altimetry products from Jason-2/PISTACH and AltiKa/PEACHI are considered to offer better estimation of significant wave height (SWH) over coastal oceans. In selecting the appropriate SWH, Jason-2/PISTACH from MLE4, Oce3 and Red3 retracking algorithms are examined, with respect to the limited data from Acoustic Doppler Current Profiler. The results in this study indicate that the Oce3 algorithm is the appropriate retracker. Unfortunately, it is only available for a Jason-2/PISTACH product, not for AltiKa/PEACHI. Therefore, this study uses the improved SWH from Red3 retracker, recorded as the second appropriate retracker, in the study of wave energy resource. The Malaysian sea is dominated by low SWH (0.5–1 m) and wave period (4–5.5 s). High wave energy during the strong monsoon season can be harvested, with wave energy during a northeast monsoon ranging from 8 to 20 kW/m, and between 4 and 5 kW/m during a southwest monsoon. Ten out of 14 zones are recorded as high energy zones, producing the energy storage more than 40 MW h/m. The Malaysian sea has a potential of continuous wave energy throughout the year from the variability of SWH exceeding the minimum requirement of SWH for several wave energy converters (e.g. C5 Wave Star) to be operated.

**Keywords** Satellite altimetry · Retracked significant wave height · Waveform retracking · Wave energy · Malaysian sea

## Introduction

With the emerging of coastal altimetry products enabling novel applications in coastal waters, ocean energy resources can be better quantified near coasts (Goddijn Murphy et al. 2015). Issues regarding the satellite altimetry data over coastal ocean have been discussed in various literatures (Gommenginger et al. 2011; Idris et al. 2014; Passaro et al. 2014; Idris et al. 2017), and in the book of *Coastal Altimetry* (Vignudelli et al. 2011). The relatively coarse spatial footprint of the satellite

(7 km for the Jason series) creates signal corruption, and difficulties in corrections are generally considered a key constraint of the altimeters for coastal studies. This results in the data rejection when near coasts, typically within 10 km from the coastline (Idris et al. 2014).

Several projects have been established enhancing the satellite altimetry data over coastal oceans, including the projects of the Coastal and Hydrology Altimetry product (PISTACH), and the Prototype for Expertise on AltiKa for Coastal, Hydrology and Ice (PEACHI). Through these projects, various data processing protocols (waveform retracking) and geophysical corrections specialised for coastal oceans have been successfully developed. Waveform retracking is an efficient signal post-processing performed to optimise the accuracy of the geophysical estimation (i.e. Significant Wave Height, SWH) based on the physical or empirical retracking algorithms (Gommenginger et al. 2011).

In addition to the advancement of data processing, the advanced altimetric technologies have been developed to perform better near the coast. The AltiKa altimeter on-board, the SARAL satellite and Synthetic Aperture Radar (SAR) on-board, the Cryosat-2, the Sentinel-3A and the Sentinel-

---

This article is part of the Topical Collection on *Geo-environmental integration for sustainable development of water, energy, environment and society*

---

✉ Nurul Hazrina Idris  
nurulhazrina@utm.my

<sup>1</sup> Department of Geoinformation, Faculty of Built Environment and Surveying, Universiti Teknologi Malaysia, 81310 Johor Bahru, Malaysia

<sup>2</sup> Geoscience and Digital Earth Centre, Research Institute for Sustainability and Environment, Universiti Teknologi Malaysia, 81310 Johor Bahru, Malaysia

3B have been established to operate in finer spatial resolution (and other several attributes), promising improved performance in coastal waters (Raney 1998; Raynal et al. 2018).

Those coastal altimetry products are freely available to various users for studying coastal ocean environments, including the ocean wave renewable energy. The potential of ocean energy resources in Malaysian seas includes the wave energy, tidal energy, salinity gradient and ocean thermal energy conversion (Yaakob et al. 2016). Of the aforementioned ocean energy resources, wave energy has an enormous exploration potential (Zubaidah et al. 2006). Although Malaysian seas are considered a low wave climate environment (Mirzaei et al. 2014; Yaakob et al. 2016), the occurrence of seasonal monsoons and the geographical location itself possibly provide continuous wave energy resources. With the seasonal monsoon generating high waves, wave energy could potentially be harvested (Mirzaei et al. 2014). It could also be advantageous for any installation of wave energy converter, safe from the impact of high waves and damaging storms.

Studies have been conducted to assess the wave energy resources in various regions (Goddijn Murphy et al. 2015; Wan et al. 2015; Bernhoff et al. 2006; Stopa et al. 2013; Kumar and Anoop 2015). Assessment is based on the oceanographic buoys data (Muzathik et al. 2010; Muzathik et al. 2011), the numerical wave models (Mirzaei et al. 2014; Zheng and Li 2011; Zheng et al. 2011) and the satellite altimetry (Goddijn Murphy et al. 2015; Wan et al. 2015; Yaakob et al. 2016; Pontes et al. 2009).

In the Malaysian sea, Muzathik et al. (2010) report the potential of wave energy along the east coast of Peninsular Malaysia. Based on the oceanographic buoys data, the averaged wave energy is up to 6.5 kW/m, and the energy storage about 18 MW h/m. These values are supported by Wan Nik et al. (2010), who found the wave energy ranging from 0.15 to 6.49 kW/m, and the storage about 17.9 MW h/m. Although both studies contribute towards the overview of Malaysian renewable energy, the data from buoys are limited from the spatial and temporal coverages. Therefore, it is inadequate to represent the whole area of interest; in this case, the Malaysian seas.

Mirzaei et al. (2014) conducted the wave energy assessment using the WAVEWATCH-III numerical wave model over the east coast of Peninsular Malaysia. Their results indicate that the wave energy over the northern region is much more energetic (2.6–4.6 kW/m) than those of the southern region (0.5–1.5 kW/m) of the coast. This is from the sheltering effects of the multiple islands between both regions. In addition, the wave energy is higher during the northeast monsoon than the other seasons.

An alternative approach of satellite altimetry in assessing wave energy in the Malaysian sea was reported by Yaakob et al. (2016). They used gridded data in  $0.25^\circ \times 0.25^\circ$  from the Radar Altimetry Database System (RADS) to get the

comprehensive spatial and temporal coverage of data for all sea zones. They report that the average wave energy and storage in Malaysian seas are between 1.41–7.92 kW/m and 7.1–69.41 MW h/m, respectively. However, it is noticed that data from RADS are not specialised for coastal oceans. That is, the data coverage is sparse (in  $0.25^\circ \times 0.25^\circ$ ), and the SWH and wind speed parameters are not improved using any coastal waveform retracers like Red3 and Oce3 (AVISO 2010). This may result in uncertainty in the measurements when near the coastline and/or islands.

In assessing the wave energy resources, two major parameters are the SWH and the wave period. In the Malaysian sea, a satellite altimeter offers valuable SWH data because the buoy measurement data are limited and rare in both number and geographical distribution (Yaakob et al. 2016). However, the wave period is not routinely measured by the altimetry. The development of algorithms to derive the wave period from satellite altimetry has been reported by several researchers (Kshatriya et al. 2005; Govindan et al. 2011; Gommenginger et al. 2003; Hwang et al. 1998). The method from Hwang et al. (1998) is marked as the most appropriate for the Malaysian sea because the estimated period has a good agreement with the buoy measurements (Yaakob et al. 2016).

This study assesses the wave energy resources of the Malaysian sea using the improved satellite altimetry data for coastal oceans. Goddijn Murphy et al. (2015) recommend that the AltiKa and the improved coastal altimetry data from previous missions can potentially explore wave energy resources all over the globe. However, such a study has never been conducted for Malaysian seas, thus becoming the motivation of this study.

## Study area and data

The coast of Peninsular Malaysia and the East Malaysia (Sabah and Sarawak basin) are considered in this study (Fig. 1). The area is within the Exclusive Economic Zone of Malaysia facing the South China Sea and Strait of Malacca. It lies above a continental shelf, with an average water depth of 200 m and contains many islands. The coastal topographies are complex including various coastal features such as islands, beaches, mangroves and corals. The area has a potential for wave energy (Yaakob et al. 2016) because it is exposed to the seasonal monsoon each year, receiving strong winds, waves and rains (Gan et al. 2006).

In this study, two high-resolution altimetric data, Jason-2 (in 20 Hz) and SARAL/AltiKa (in 40 Hz), are utilised. The parameter of interests is the SWH and wind speed. The data are gathered from coastal products optimised for coastal applications using waveform retracking approach (Fernandes et al. 2003; Gommenginger et al. 2011; Idris and Deng 2012; Kuo et al. 2011). This alternative coastal product is

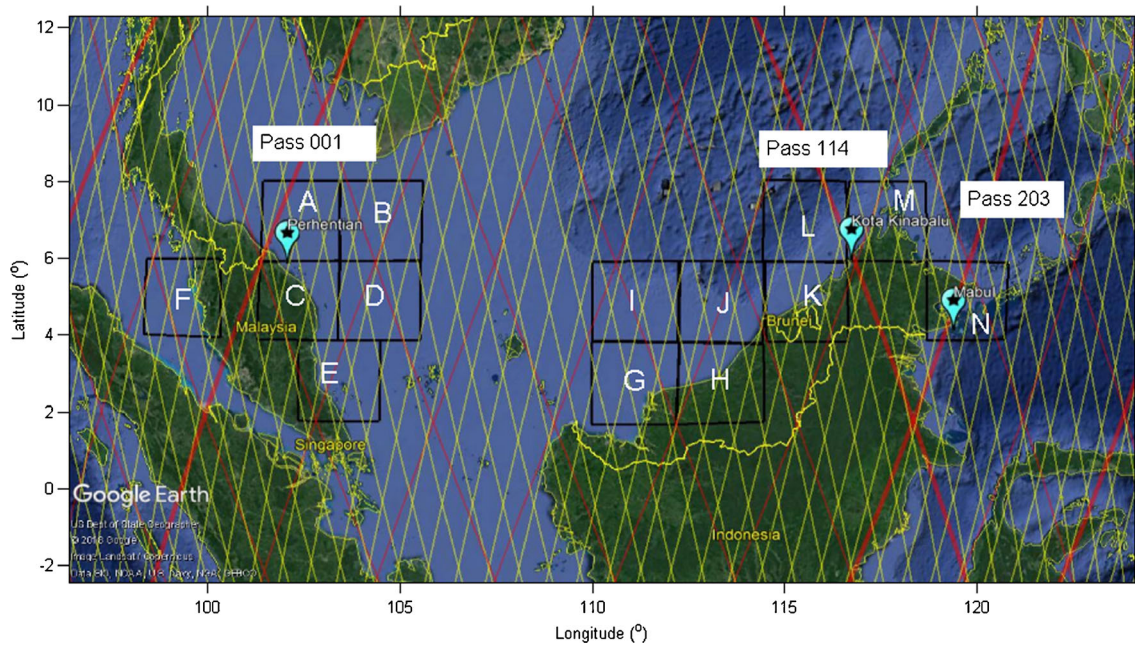


**Figure 1** Study area around the coast of Peninsular and East Malaysia (depicted from Google Earth). The satellite altimetry tracks of Jason-2 (in red) and SARAL/AltiKa (in yellow) are also shown. For validation purposes, the ADCP stations at Perhentian, Kota Kinabalu and Mabul are

shown in blue star, and the Jason-2 satellite passes 001, 114 and 203 are shown in bold red lines. The selected 14 zones for the assessment of wave energy resources are denoted as A–N

utilised as a response to the issue of altimetry over coastal ocean (Gommenginger et al. 2011), where the measurements near the coasts have been largely discarded as ‘bad data’. With the coastal altimetry data products, accurate ocean geophysical information (SWH, wind speed and sea level) can be retrieved over coastal oceans (Andersen and Scharroo 2011; Cipollini et al. 2009).

The Jason-2/PISTACH and AltiKa/PEACHI from December 2014 to 2016 are retrieved from the Archiving, Validation and Interpretation of Satellite Oceanographic ftp site (<ftp://avisoftp.cnes.fr>). These datasets are purposely used to assess the wave energy resources over the experimental region. The improved SWH from coastal retracers are retrieved. They are from Red3 and Oce3 retracers for the PISTACH product, and Red3 and BAGP retracers for the PEACHI product. The standard ocean retracker of MLE4 is also available for both products. Details about the retracking algorithms can be found in AVISO (2010) and Valladeau et al. (2015). Note that the coastal retracers available in both products are different.

The wind speed data are also retrieved from the coastal altimetry products. They are derived empirically through a mathematical relationship with the Ku-band backscatter coefficient and the SWH using the Gourrion algorithm (Gourrion, 2002). The wind speed model function is evaluated for 10 m above the sea surface and is considered to be accurate to 2 m/s (AVISO 2010).

For validation purposes, limited wave height data from the Acoustic Doppler Current Profiler (ADCP) are available from

January 2009 to 2010. Therefore, Jason-2/PISTACH data from a similar duration (January 2009–2010) are also retrieved to assess the quality of altimetric SWH against ADCP. It is noted that AltiKa was launched on February 2013; thus, comparing with available ADCP is impossible. The validation against ADCP is conducted over three stations: Perhentian, Kota Kinabalu and Mabul (see Fig. 1 and Table 1). The nearest distance of Jason-2 passes to the ADCP station shown in Table.1.

### Methodology

To ensure that the most optimised retracked SWH is utilised in the computation of wave energy, validation of retracked SWH against ADCP is conducted. The validation is conducted by computing the number of valid results of retracking algorithms, root mean square (RMS) error, median absolute deviation (MAD) and correlation. In the assessment, the along-track altimetry data are averaged within every 5-km distance bands. The averaged SWH data are then compared with the ADCP SWH. The results are discussed in the ‘Assessing the appropriate retracker for significant wave height’ section.

The most appropriate retracked SWH is then used to compute the wave energy. The wave power can be expressed as follows (Goddijn Murphy et al. 2015; Yaakob et al. 2016):

$$P = \frac{\rho g^2}{64\pi} H_s^2 T_e = 0.49 H_s^2 T_e \tag{1}$$

**Table 1** Description of ADCP stations used for validation purposes

| ADCP stations | Coordinate    |                | ADCP distance (km) |   |
|---------------|---------------|----------------|--------------------|---|
|               | Latitude (°N) | Longitude (°E) | To the coast       | To the nearest Jason-2 satellite track (pass no.) |
| Perhentian    | 5.9133        | 102.7130       | 17.26              | 71 (001)  |
| Kota Kinabalu | 6.0405        | 116.1094       | 0.17               | 14 (114)  |
| Mabul         | 4.2593        | 118.6329       | 13.67              | 19 (203)  |

where  $P$  is the wave power per unit of crest length (kW/m),  $H_s$  is the SWH (in unit meter),  $T_e$  is the wave period (in unit second),  $\rho$  is the density of seawater (assumed to be  $1025 \text{ kg/m}^3$ ) and  $g$  is the gravitational acceleration. Although the expression in Eq. (1) is suitable for the deep ocean, previous study by Yaakob et al. (2016) indicate that it is also applicable for the coastal ocean around Malaysia.

Unlike SWH,  $T_e$  cannot be measured with satellite altimeters; therefore, the wave period is calculated using an equation from Hwang et al. (1998). In the Hwang method, the peak period of the wave field,  $T$  (in unit second), is related to wind speed,  $U$  (in unit m/s), and significant wave height,  $H_s$ . It is expressed as follows:

$$\frac{U}{gT} = 0.048 \left( U^2 / (gH_s) \right)^{0.67} \quad (2)$$

where  $g$  is gravitational acceleration. The value of wind speed,  $U$ , and significant wave height,  $H_s$ , can be obtained from satellite altimetry.

According to Yaakob et al. (2016), Eq. (2) is the best method for Malaysian coastal water for several reasons. First, it is aligned with the most wave energy converter (WEC) developers approach, showing their WEC power production by means of a power matrix in terms of  $H_s$  and  $T$ . Second, comparison with buoy data indicates a good agreement among both datasets, where the correlation coefficient of the wave period,  $T_e$ , exceeds 0.8. However, a high RMS error (0.993 s) is found from large variations when different data processing procedures are used in the Hwang et al. (1998) algorithm.

To estimate the total energy resource at each zone (Fig. 1), the annual wave energy density,  $P_{\text{density}}$ , and the annual energy production,  $E_{PT}$  are calculated.  $P_{\text{density}}$  is computed based on the probability occurrence in the wave scatter table in the 'Wave scatter diagram' section. By assuming the  $P_{\text{density}}$  corresponds to the sea state in different ranges of SWH and wave period, regarding its probability of occurrence, the annual  $P_{\text{density}}$  in each zone can be expressed as follows (Yaakob et al. 2016; Kofoed et al. 2013):

$$P_{\text{density}} = \sum P \times Prob \quad (3)$$

where  $P$  is the amount of wave energy contributed in the relative SWH and the wave period (in unit KW/m), and  $Prob$  is the relative SWH and wind period probability of occurrence. The total energy storage,  $E_{PT}$  per unit zone (in unit MW h/m) is calculated by multiplying the annual  $P_{\text{density}}$  with the number of hours in a year, approximately 8766 h. It can be expressed as follows (Zheng et al. 2013):

$$E_{PT} = P_{\text{density}} \times 8766 \quad (4)$$

### Assessing the appropriate retracker for significant wave height

The PISTACH and PEACHI products from satellite altimeters offer several options of improved SWH data for coastal oceans. Therefore, it is important to use the most appropriate SWH before computing the wave energy. An assessment is conducted to identify the quality of improved SWH from the standard retracker of MLE4, and the coastal retrackers of Red3 and Oce3 from Jason-2/PISTACH product. The assessment is conducted by computing the number of valid results of the retracking algorithms, and RMS error, MAD and temporal correlation against ADCP data along selective satellite passes (Table 1). These values are computed and averaged over several distance bands from the coastline.

To compare with ADCP data, the closest date and time of both datasets are searched. This is important because the ADCP data are available hourly, while the Jason-2 data are available approximately every 10 days.

To decide the appropriate retracker, a systematic ranking (Table 2) is developed to rate the performance of retrackers. Each assessment of each distance band is given a rank from one to ten, where one indicates the worst performance and ten indicates the best performance. The rank values are then summed to identify the appropriate retracker. Based on Table 2, a high rank is given to the retracker with a high fraction of valid results and correlation, and low RMS error and MAD. Since it is well known that altimetry data over coastal are usually flagged as bad due to land contamination, an appropriate retracker that capable of recovering more valid results near the coast with the high accuracy and precision is sought. The fraction of valid result indicates the capability of a

**Table 2** Ranking system to identify the appropriate retracker. The fraction of valid results (in unit of %) is scaled to 0–1 for consistency with the other variables

| Rank | Fraction of valid results | RMS error (m) | MAD (m)   | Correlation |
|------|---------------------------|---------------|-----------|-------------|
| 1    | 0.00–0.10                 | 0.91–1.00     | 0.91–1.00 | 0.00–0.10   |
| 2    | 0.11–0.20                 | 0.81–0.90     | 0.81–0.90 | 0.11–0.20   |
| 3    | 0.21–0.30                 | 0.71–0.80     | 0.71–0.80 | 0.21–0.30   |
| 4    | 0.31–0.40                 | 0.61–0.70     | 0.61–0.70 | 0.31–0.40   |
| 5    | 0.41–0.50                 | 0.51–0.60     | 0.51–0.60 | 0.41–0.50   |
| 6    | 0.51–0.60                 | 0.41–0.50     | 0.41–0.50 | 0.51–0.60   |
| 7    | 0.61–0.70                 | 0.31–0.40     | 0.31–0.40 | 0.61–0.70   |
| 8    | 0.71–0.80                 | 0.21–0.30     | 0.21–0.30 | 0.71–0.80   |
| 9    | 0.81–0.90                 | 0.11–0.20     | 0.11–0.20 | 0.81–0.90   |
| 10   | 0.91–1.00                 | 0.00–0.10     | 0.00–0.10 | 0.91–1.00   |

retracker to recover more datasets, thus reducing the no-data gap near coastline. The correlation coefficient merits to find the precision of the along-track retracked SWH, while the RMS and MAD merit to finding the accuracy of SWH.

Figure 2 shows the analysis of MLE4, Oce3 and Red3 retrackers along selective Jason-2 passes near ADCP stations. The analysis values are averaged over the distance band to the coast.

Based on the results in Fig. 2, the analysis within band 0–5 km for all passes (Fig. 2a–c) and band 5–10 for pass 001 (Fig. 2a) is unreliable because of data unavailability. A similar issue has been reported by several researchers (Deng and Featherstone 2006; Idris and Deng 2012; Gommenginger et al. 2011), in which the altimetric signals are perturbed by emerged land when near the coastline. When the altimeter footprint is partly over the ocean and partly over the land, the reflective properties are the relative proportion of sea and land areas (Gommenginger et al. 2011). This produces an inaccurate geophysical estimation over the coastal region, typically within the distance of comparable size of the altimeter footprint (7 km for Jason-2) (Idris and Deng 2012).

The results in this section (Fig. 2) show that the value of correlation is low (< 0.5) for all retrackers in the three stations. The Oce3 retracker has the maximum correlation of 0.46, while the MLE4 and Red3 retrackers have 0.45 and 0.39, respectively. This suggests that the improved SWH from these retrackers is less coherent. The reason potentially responsible is that the distance between the ADCP stations to the nearest satellite passes is huge, ranging from 13 to 71 km (Table 1). This may produce an incoherency because of the time lag, and the fact that wave signals in the coastal region are more complex than in the deep ocean, where they tend to be larger, of shorter wavelength, and possibly nonlinear in dynamical wave motion. Although the value of correlation is low, the analysis of RMS error and MAD indicates that the discrepancy among

the altimetric improved SWH with ADCP-SWH is small (< 0.6 m), suggesting that the improved SWHs are reliable.

Table 3 shows the summary of ranking value for all retrackers over the three ADCP stations. It is found that the Oce3 retracker outperforms the MLE4 and Red3 retrackers in all three stations. This is indicated by the highest total ranking values of Oce3 retracker. The results also indicate that in two out of three stations, the Red3 retracker is more appropriate than those of the MLE4 retracker. This finding is supported by Idris (2014), where the Oce3 retracker is found superior to those of Red3 and MLE4 retrackers over the Great Barrier Reef, Australia. On the other hand, the Red3 retracker outperforms the MLE4 retracker in four out of six passes.

In this study, the assessment is only conducted for the Jason-2/PISTACH product. Concerning the performance of SARAL/AltiKa, recent studies (Sepulveda et al. 2015; Goddijn Murphy et al. 2015) confirmed that the SWH from AltiKa is more accurate near the coast than the previous altimeters (the Jason series), particularly at a low SWH. Unlike the altimeter of previous missions, the AltiKa advanced technology offers a higher frequency, larger bandwidth, smaller antenna beam width, higher pulse repetition frequency and echo tracking, thus contributing to improved performance in coastal water (Verron 2013). The authors' previous study of the Malaysian coast (Abdullah and Idris 2018) identified the standard MLE4 retracked data from AltiKa can provide measurements as close as 3 km from the coastline with data coverage up to 88%.

It can be summarised that the SWH from AltiKa can provide good measurements over the coastal ocean, and the Jason-2/PISTACH from Oce3 retracker is the appropriate retracker for accurate SWH retrieval. However, it is realised that the Oce3 retracker is limited to Jason-2/PISTACH product. Therefore, to compute the wave energy, the improved SWH from Red3 is used instead of Oce3, because it is available from both the Jason-2/PISTACH and AltiKa/PEACHI data.

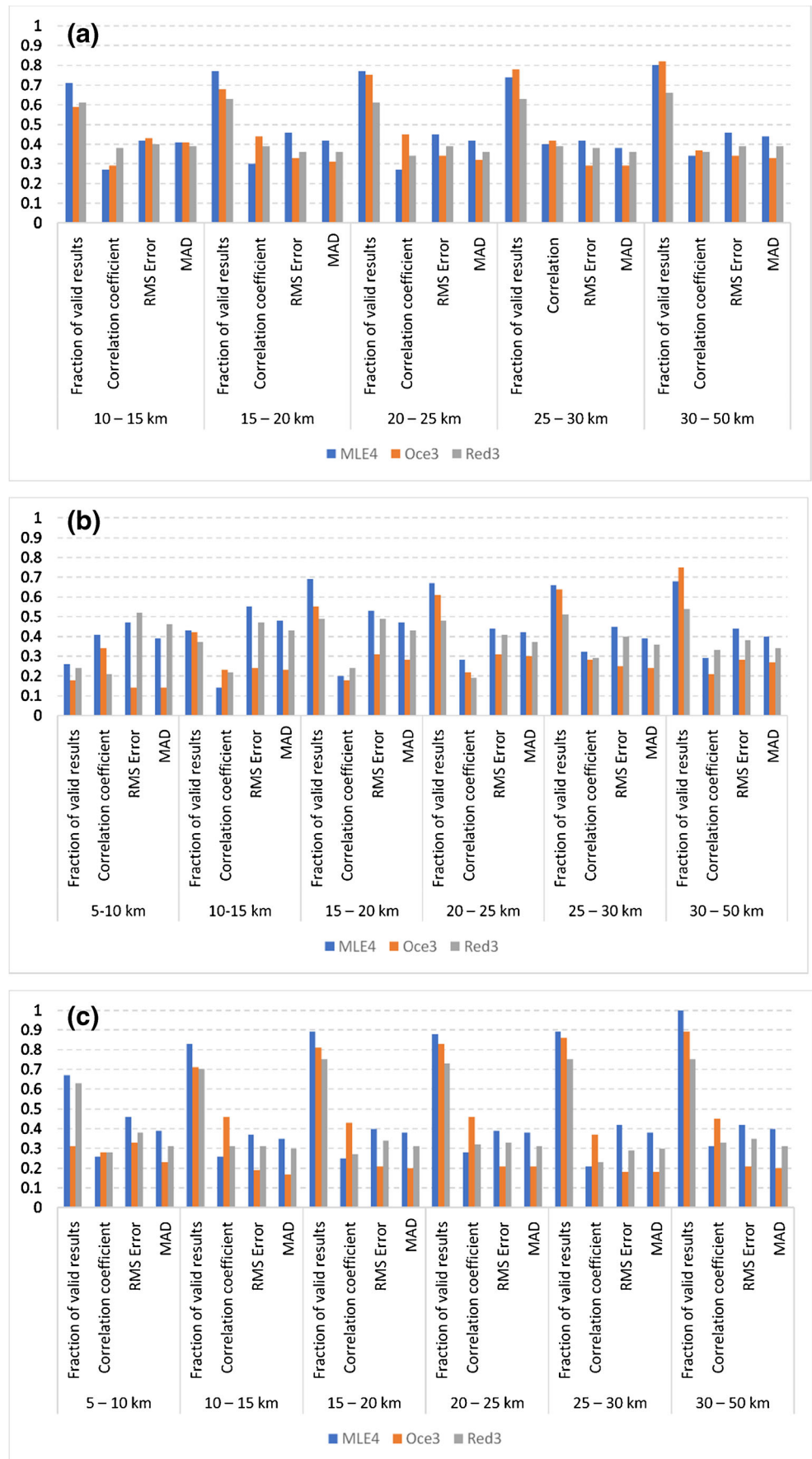
Note that the performance of retrackers might vary depending on the coastal topography. The results presented in this section are only applicable to the tested regions, in this case the Malaysian seas. If one would apply the similar approach, the appropriate retracker should be examined.

## Assessing wave energy resources in Malaysia

### Wave scatter diagram

Fourteen specific zones in  $2^\circ \times 2^\circ$  are selected to investigate the potential of wave power in Malaysia (Fig. 1). Examples of scatter diagrams are shown in Tables 4, 5 and 6 to represent the composition of wave energy resources for wave height and wave period from altimetric data over 2 years. Since

**Fig. 2** The analysis of MLE4, Oce3 and Red3 retrackerers along selective Jason-2 passes near ADCP stations of Perhentian (a), Mabul (b) and Kota Kinabalu (c)



Malaysian seas comprise of various coastal topographies (including beaches, mangroves, corals and islands), the composition of wave energy resources for wave height and wave period over the respective zones can be learnt. The annual probability distribution of SWH and the wave period are tabulated in seven intervals of SWH and thirteen intervals of wave period. The number within each cell represents the occurrences of sea states whose SWH and wave period fall within the corresponding range. The annual probability is given in part per thousands; thus, implying that a value of 60 would represent a probability of 0.060 or 6.0%.

Based on the results, the dominant SWH and wave period of 0.5–1 m and 4–5 s, respectively, are observed for most of the zones. Several zones (B, I and L, in Figs. 4, 5 and 6) recorded a slightly higher composition of SWH and wave period (1–1.5 m and 5–6 s). These zones are located at the off-shore of the South China Sea (Fig. 1). In general, wave dynamics in the off-shore is greater than those in the near-shore. This is because the waves propagate in the off-shore are unaffected by the sea bottom. However, as they move towards the shoreline, they eventually reach a point from which the seabed starts to affect their propagation through refraction, shoaling and bottom friction. From this point onwards, waves dissolve part of their energy with the seabed (Muzathik et al. 2010).

This demonstrates that Malaysian seas have a low climate condition with dominant SWH between 0.5 and 1.5 m and wave period between 4 and 6 s. The value of SWH well agreed with findings from Yaakob et al. (2016). However, the value of the wave period found in this study is somewhat lower than those of Yaakob et al. (2016), who found the wave period is between 5 and 7 s. The slight discrepancy may be because they computed the probability occurrence from 10 years of data, while this study uses only 2 years of data. It is noted that longer time series data should be considered in the future to obtain better results. It is also noticed that Yaakob et al. (2016) used altimetry data from RADS, which is not specialised for the coastal ocean. The data suffers from data loss and is flagged as bad typically at 10 km from the coastline because of the difficulties in the corrections and issues of land contamination in the altimetric footprint (Gommenginger et al. 2011). The spatial resolution of the data is considered low, providing measurements in

$0.25^\circ \times 0.25^\circ$  grid, when compared with the data used in this study (20 Hz for Jason/PISTACH and 40 Hz for AltiKa/PEACHI). As recommended by various researchers (Cipollini et al. 2010; Cipollini et al. 2008; Gommenginger et al. 2011), the coastal altimetry product should be considered when conducting any coastal applications to obtain better results.

The results in this section recommend that the Malaysian seas require WEC that practically can gain more energy at a low SWH and wave period. This is valuable information, especially for WEC developers, to design, develop and select devices that perform the best in their area of interest. The minimum and maximum wave height is the main working requirement of a device (Yaakob et al. 2016). Table 7 summarises the wave energy converters along with their minimum wave height requirements to operate that are currently available at the commercial stage. It seems that the Attenuator WEC type, for instance the Pelamis and C5 Wave Star, is suitable for the Malaysian seas since it can be operated at the minimum SWH of 0.5 m.

### Comparison of wave height, wave period and wave energy with ADCP data

The scatterplot of wave height, wave period and wave energy derived from the altimeter and ADCP data is presented in Fig. 3. The regression lines and residual curves are also shown in Fig. 3. The samples are selected based on the nearest distance between the altimeter and ADCP locations, and the closest temporal among both datasets. Due to limited ADCP data, only eleven samples are available for comparison.

The results indicate that the correlation coefficient of wave height (Fig. 3a) and wave energy (Fig. 3e) exceeds 0.6, while for the wave period (Fig. 3c), the correlation is only 0.47. The residual curves of wave height (Fig. 3b), wave period (Fig. 3d) and wave energy (Fig. 3f) are found concentrated under the lower digits of y-axis between  $-0.2$  m to  $0.2$  m,  $-2$  s to  $2$  s and  $-1$  to  $1$  kW/m, respectively, suggesting small discrepancy among both datasets. Also, generally there are no obvious pattern can be observed on those residual curve figures. These suggest that the regression lines show the accurate relationship of the datasets.

The RMS error of the wave height and wave energy is considered low at 0.05 m and 0.45 kW/m, respectively. However, the RMS error of wave period is relatively high, at 1.16 s. These results mimic studies by Yaakob et al. (2016) and Muzathik et al. (2010), which found a high RMS error of wave period at 0.993 s and 0.646 s, respectively. These values are considered high because of the difference in data processing procedures to extract wave period parameter. In addition, the wave period is an unstable quantity (Hwang et al. 1998; Yaakob et al. 2016).

**Table 3** The total rank of the retracers at the three ADCP stations. The highest rank at each station is indicated in italics

| Stations      | MLE4 | Oce3       | Red3 |
|---------------|------|------------|------|
| Perhentian    | 118  | <i>130</i> | 125  |
| Mabul         | 128  | <i>149</i> | 123  |
| Kota Kinabalu | 152  | <i>177</i> | 157  |

**Table 4** Annual wave scatter occurrence in zone B

| SWH (m) | Wave period (s) |     |     |     |     |     |     |     |      |       |       |       |      |
|---------|-----------------|-----|-----|-----|-----|-----|-----|-----|------|-------|-------|-------|------|
|         | 1–2             | 2–3 | 3–4 | 4–5 | 5–6 | 6–7 | 7–8 | 8–9 | 9–10 | 10–11 | 11–12 | 12–13 | > 13 |
| 0.0–0.5 | 10              | 30  | 44  | 18  | 6   | 2   | 1   |     |      |       |       |       |      |
| 0.5–1.0 |                 |     | 30  | 125 | 69  | 21  | 10  | 6   | 3    | 2     | 0.3   |       |      |
| 1.0–1.5 |                 |     |     | 14  | 151 | 71  | 12  | 7   | 4    | 3     | 2     | 1     | 1    |
| 1.5–2.0 |                 |     |     |     | 5   | 100 | 52  | 7   | 4    | 3     | 2     | 1     | 1    |
| 2.0–2.5 |                 |     |     |     |     | 6   | 74  | 35  | 4    | 1     | 1     | 0.8   | 0.5  |
| 2.5–3.0 |                 |     |     |     |     |     | 12  | 31  | 7    | 1     | 0.1   | 0.1   |      |
| > 3.0   |                 |     |     |     |     |     |     | 4   | 2    | 2     | 0.2   |       |      |

### Monthly variability of wave period and wave energy

The monthly variation of SWH and the wave period from satellite altimetry is shown in Fig. 4, and the monthly variation of the wave energy is presented in Fig. 5.

Monthly variation of SWH characterised the real environment of the Malaysian sea, where the variability is strongly affected by the monsoon seasons. During the northeast monsoon (November–February), high SWH and wave periods are experienced. The SWH and wave period exceed 1.3 m and 5.8 s, respectively, during this season. This results in high wave energy resources between 8 and 20 kW/m.

During the southwest monsoon (June–September), the variation of monthly averaged SWH is 0.8–1 m, while the averaged wave period is 5–5.5 s. This produces wave energy between 4 and 5 kW/m.

Comparable results are observed by Muzathik et al. (2010) and Muzathik et al. (2011), who recorded a high SWH and wave period variations during the northeast monsoon season.

Results from Figs. 4 and 5 expose a potential of wave energy throughout the year, ranging from 2.5 to 20 kW/m. There is a wide range because there is large variability of SWH and wave periods throughout the year exceeding the minimum requirement of SWH for several WEC to operate. For instance, the C5 Wave Star WEC (Kramer et al. 2011) and

Pelamis Wave Power (Power 2017) can operate efficiently with a minimum SWH of 0.5 m (see Table 7).

### Potential zones of wave energy

For better understanding the potential wave energy resources in Malaysian sea, two variables are discussed: (1) wave energy density; (2) and wave energy storage. Figure 6 illustrates the annual average wave energy density and total wave energy storage resources per unit area for each selected zone. Calculating the storage energy provides information for designing the technical and operating system of WEC (Zheng et al. 2016). The integration of energy storage and the technologies is important to improve the potential for flexible energy demand and ensure that excess renewable energy can be stored for use at a later time (Spataru et al. 2014).

Based on Fig. 6, the estimated wave energy density in the Malaysian sea is between 1.9 and 7.7 kW/m. This finding well agrees with the studies of Yaakob et al. (2016) and Zheng et al. (2013), who found the wave energy density in the South China Sea ranges between 1 and 7 kW/m.

Several studies (Ren et al. 2009; Zheng et al. 2013) suggest that the area with wave energy density  $\geq 2$  kW/m is considered an area with available wave energy, while the area with density  $\geq 20$  kW/m is considered a rich zone. Referring to Fig. 6,

**Table 5** Annual wave scatter occurrence in zone I

| SWH (m) | Wave period (s) |     |     |     |     |     |     |     |      |       |       |       |      |
|---------|-----------------|-----|-----|-----|-----|-----|-----|-----|------|-------|-------|-------|------|
|         | 1–2             | 2–3 | 3–4 | 4–5 | 5–6 | 6–7 | 7–8 | 8–9 | 9–10 | 10–11 | 11–12 | 12–13 | > 13 |
| 0.0–0.5 | 15              | 43  | 52  | 17  | 5   | 1   | 0.4 |     |      |       |       |       |      |
| 0.5–1.0 |                 | 0.3 | 30  | 104 | 63  | 23  | 13  | 6   | 2    | 1     | 0.2   |       |      |
| 1.0–1.5 |                 |     | 0.1 | 10  | 111 | 69  | 17  | 8   | 7    | 4     | 2     | 1     |      |
| 1.5–2.0 |                 |     |     | 0.2 | 6   | 75  | 42  | 11  | 2    | 1     | 1     | 1     | 1    |
| 2.0–2.5 |                 |     |     |     |     | 6   | 45  | 32  | 11   | 1     | 0.3   | 0.1   |      |
| 2.5–3.0 |                 |     |     |     |     |     | 6   | 34  | 26   | 9     | 1     | 0.1   |      |
| > 3.0   |                 |     |     |     |     |     | 0.1 | 7   | 33   | 30    | 11    | 2     | 0.2  |



**Table 6** Annual wave scatter occurrence in zone L

| SWH (m) | Wave period (s) |     |     |     |     |     |     |     |      |       |       |       |      |
|---------|-----------------|-----|-----|-----|-----|-----|-----|-----|------|-------|-------|-------|------|
|         | 1–2             | 2–3 | 3–4 | 4–5 | 5–6 | 6–7 | 7–8 | 8–9 | 9–10 | 10–11 | 11–12 | 12–13 | > 13 |
| 0.0–0.5 | 12              | 38  | 44  | 13  | 7   | 3   | 1   |     |      |       |       |       |      |
| 0.5–1.0 |                 |     | 41  | 137 | 63  | 17  | 10  | 7   | 4    | 2     | 1     | 0.1   |      |
| 1.0–1.5 |                 |     |     | 23  | 172 | 82  | 22  | 7   | 4    | 3     | 2     | 1     | 1    |
| 1.5–2.0 |                 |     |     |     | 10  | 105 | 44  | 14  | 3    | 2     | 1     | 1     | 0.7  |
| 2.0–2.5 |                 |     |     |     |     | 9   | 43  | 12  | 4    | 2     | 0.2   | 0.2   | 0.6  |
| 2.5–3.0 |                 |     |     |     |     |     | 7   | 13  | 2    | 1     | 0.1   | 0.1   |      |
| > 3.0   |                 |     |     |     |     |     |     | 2   | 3    | 1     | 1     | 0.4   | 0.6  |

most of the zones in the Malaysian seas can be considered an area with available wave energy, except at zone F, where the density is < 2 kW/m. Zone F is located at the Strait of Malacca where the ocean variability differs from that of the South China Sea.

In this study, the energy resources are presented in three categories: high, intermediate and low energy zones (Yaakob et al. 2016; Zheng et al. 2013). A high energy zone consists of total energy storage greater than 40 MW h/m, while intermediate and low energy zones consist of energy storage between 20 and 40 MW h/m and less than 20 MW h/m, respectively. The low energy zones include zone F, located at the Strait of Malacca, and the intermediate energy zones include zones K, M and N, which are in East of Malaysian waters. The high energy zones include zones A–E, zones G–J and zone L. Zones A–E are situated at the east coast of Peninsular Malaysia, while zones G–J and L are situated in East Malaysian waters. The high energy zones are expected to generate up to 65.6 MW h/m of energy, agreeing with the study by Yaakob et al. (2016) that records the energy up to 69.41 MW h/m in high zones. Nevertheless, when compared

with findings of Yaakob et al. (2016), the high energy zones found in this study are much broader, covering all five zones along the east coast of Peninsular Malaysia and five zones within East Malaysian waters. The difference is mainly from the improvement in the estimated SWH, which is specialised for the coastal oceans.

### Discussions

The findings from this study clearly provide a scientific advancement in terms of wave knowledge in coastal seas, particularly in Malaysia. It exposes that wave data can be accurately retrieved from the specialised coastal altimetry data products such as PISTACH and PEACHI. Despite a frequent and dense coverage of data, coastal altimetry products offer reliable and accurate datasets over coastal zones. This overcomes the lacking in existing in situ techniques for studying ocean waves. The in situ buoys observations are location-specific and generally sparse. It might contain instrumental errors, and the measurements might not representative of local

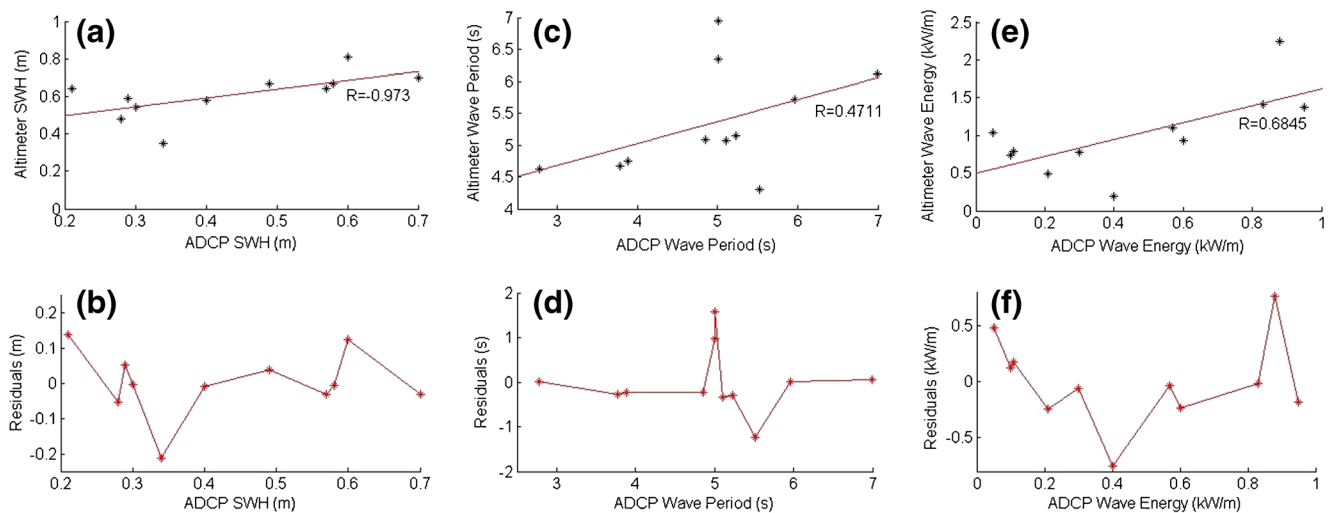
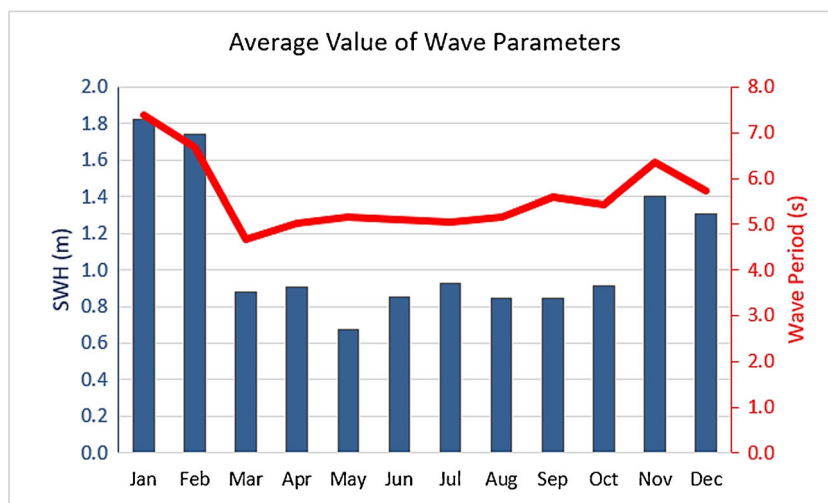


**Fig. 3** Scatterplots and residuals of wave height (a, b), wave period (c, d) and wave energy (e, f) derived from altimeter and ADCP data. The regression lines are also shown in a, c and e

**Fig. 4** Variation of monthly averaged SWH (in blue) and wave period (in red) from satellite altimetry



surrounding wave environment, such as buoys in protected areas of a harbour (Sepulveda et al. 2015). In addition, missing and invalid measurements might be identified. Therefore, quality controls are required to check and calibrate the quality of collected data before they can be applied to any coastal applications. In the South China Sea and Indian Ocean, the situation is even worse, compared with the Atlantic and Pacific, because long time series data of in situ observations are mostly unavailable (Justin and Dwarakish 2015). On the other hand, it is simply impossible to estimate the wave climate and extreme sea state without such a long time series data (Justin and Dwarakish 2015).

Other wave measurement techniques such as numerical wave modelling offer valuable information about wave climate conditions. However, drawbacks might be experienced when using such data since they are based on certain basic assumptions that may not well represent the real wave conditions. The performance of numerical wave model depends on how best the phenomena are expressed into the numerical schemes, so that more accurate wave parameters could be estimated (Justin and Dwarakish 2015). The numerical model

of WAVE WATCH III, for example, is mainly suitable for deep water regions (Bulhoes and Fernandez 2011). Applying the model in coastal zones will affect the accuracy of the coastal studies.

The results from this study reduce the gap in the existing in situ observations and numerical wave modelling. Together with the existing datasets, coastal altimetry products can be assimilated in the numerical wave modelling for better estimation of the wave climate conditions over the coastal zones.

To further understand the wave climate condition in Malaysian seas, the advanced technology of Synthetic Aperture Radar (SAR) altimetry should be considered in the future studies. However, in the case of Malaysian sea, a specialised coastal SAR retracker is required to improve the accuracy of retracked SWH. Based on our initial study, the SWH retracked by the standard SAMOSA retracker may not accurate in this region because of severe land contaminations. Although the SAR altimetry technology (e.g. on-board of Sentinel-3 satellite) offers an accurate high spatial resolution (300 m) data at along-track direction, across the satellite track, the spatial resolution ( $\sim 7$  km) is still similar to those of the

**Fig. 5** Variation of monthly averaged wave energy (in unit kW/m) from January to December

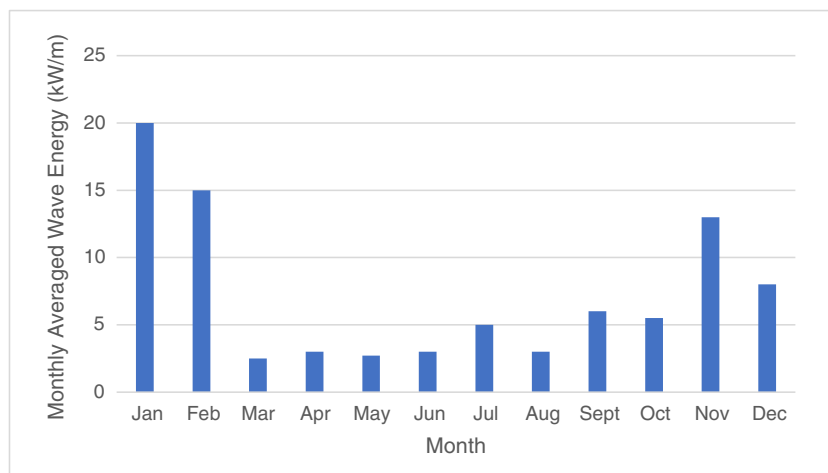
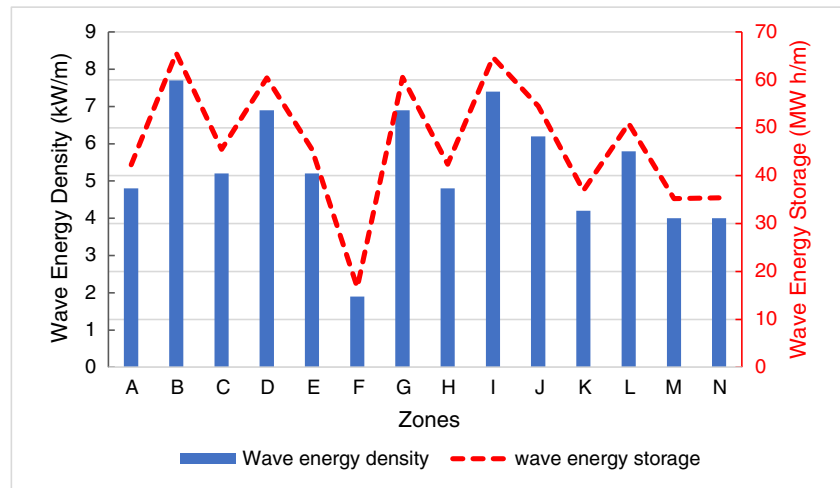


**Table 7** Examples of multi-type wave energy converter available at commercial stage, and their operation's minimum requirements

| Name/company  | Tested/deployed   | Parameters associated   | The yield of energy conversion systems                         | Reference   |
|---|---|---|--|---|
| Attenuator wave energy converter<br>Pelamis/Pelamis Wave Power                                  | UK  | Operates minimum wave height, 0.5 m<br>Operates depth at grater 50 m                              | Average yield energy 150 kW                                    | (Power 2017) <a href="https://www.pelamiswave.com/">https://www.pelamiswave.com/</a>  |
| C5 Wave Star/Wave star energy   | Denmark, 2009   | Operates minimum wave height, 0.5 m<br>Operates maximum wave height, 3.0 m<br>Operates near shore | Yield energy yield 649 MWh per year                            | (Kramer et al. 2011)  |
| Oscillating water column<br>Mutriku Wave Energy Plant   | Spain, 2011   | Shoreline   | Average yield energy 300 kW                                    | <a href="https://www.power-technology.com/projects/mutriku-wave/">https://www.power-technology.com/projects/mutriku-wave/</a>   |
| Overtopping wave energy converter<br>Seawave Slot-Cone Generator Plant                          | Norway  | Shoreline   | Average yield energy 19 kW/m                                   | (Margheritini et al. 2007)  |
| Wave Dragon/wave dragon   | Denmark 2003  | Water elevation more than 1.5 m<br>Operates at depth greater 25 m                                 | Average yield energy 50 MW                                     | (Madsen et al. 2012)  |
| Point absorber wave energy converter<br>Power buoy (PB 150)/Ocean Power Technologies<br>Wavebob | Scotland's North East coast<br>Ireland                  | Operates minimum wave height, 2 m<br>Operates at water depths of 25 to 50 m                       | Average yield energy 8.4 kWh/day<br>Average yield energy 50 kW | <a href="https://www.oceanpowertechnologies.com/pb3">https://www.oceanpowertechnologies.com/pb3</a><br><a href="https://www.engineersireland.ie/EngineersIreland/media/SiteMedia/groups/Divisions/new-energy/Wavebob-Development_of_a_Wave_Energy_Converter.pdf?ext=.pdf">https://www.engineersireland.ie/EngineersIreland/media/SiteMedia/groups/Divisions/new-energy/Wavebob-Development_of_a_Wave_Energy_Converter.pdf?ext=.pdf</a><br><a href="http://www.aquaret.com/images/stories/aquaret/pdf/device/wave.pdf">http://www.aquaret.com/images/stories/aquaret/pdf/device/wave.pdf</a> |
| IPS Buoy (AquaBuOY)/Finavera Renewables   | AquaBuOY trial at Pacific Ocean off the coast of Oregon | Operates at depth grater 50 m   |  |   |

**Fig. 6** Averaged wave energy density (in unit kW/m) and wave energy storage (in unit MW h/m) at zones A–N



conventional altimetry low-resolution mode waveforms (Dinardo et al. 2013; Thibaut et al. 2014). This implies that when the satellite track runs parallel to the shoreline, the accuracy of geophysical parameters degrades, particularly within  $\sim 7$  km from the coastline. This is because of the across-track spatial resolution is sparse ( $\sim 7$  km), similar to those of the conventional satellite altimetry (e.g. Jason series and Envisat), leading to erroneous estimation in the altimetric signals. Our initial studies found that there are severe impacts of land on the SAR altimetry waveforms, where complicated coastal waveforms are observed within 7 km from the coastlines. This is mainly due to the fact that the orientation of Malaysian coastline is parallel to certain satellite tracks. Therefore, the standard SAR retracker (e.g. SAMOSA) is less effective in this region, thus showcasing the need of coastal SAR retracker to better deal with the complicated coastal SAR waveforms. The development of coastal SAR retracker is our ongoing research.

## Conclusions

This study provides a fundamental overview on wave climate in selected zones around the Malaysian sea. Using an improved coastal altimetry data product of Jason-2/PISTACH and AltiKa/PEACHI, this study reveals that Malaysia has a low wave climate with a monthly averaged SWH and wave period between 0.7–1.8 m and 4.8–7 s, respectively. Of 14 zones, 13 zones are marked as available wave energy, with a density greater than 2 kW/m. Ten out of 14 zones are recorded as high energy, with storage greater than 40 MW h/m. Zone F, situated at the Strait of Malacca, is marked as having less potential wave energy from low energy density and storage. This is expected, because the Strait of Malacca is a semi-closed ocean, encountering small swell waves, when compared with the South China Sea. Zones A–E, located along the east coast of Peninsular Malaysia, and zones G–J and L,

located at the East Malaysia, have enormous potential for the development of wave farms. They are estimated to produce between 42 and 66 MW h/m of energy.

With such a low wave climate, an efficient and reliable device that can enable maximum energy harvesting is crucial for the Malaysian sea.

The presented technique shows the potential of applying the coastal altimetry products for exploring wave energy resources all over the globe. Advantages can be taken, but not only limited to the Jason-2 and AltiKa data, but also the previous altimeter data that are currently being reprocessed using algorithms improved for the coastal zone.

**Acknowledgements** We would like to acknowledge the AVISO data teams for kindly providing Jason-2 and AltiKa data, and the Department of Meteorological Malaysia for providing the ADCP buoys data.

**Funding information** The research is financially supported by the UTM-RUG Tier 1 (Vot 17H59), Ministry of Education Malaysia.

## References

- Abdullah NN, and Idris NH (2018) “Validation and quality assessment of sea levels from SARAL/AltiKa satellite altimetry over the marginal seas at the Southeast Asia.” In *Multi-purposeful application of geospatial data*, edited by R Rustam, 45–62. United Kingdom: IntechOpen
- Andersen OB, and Scharroo R (2011) “Range and geophysical corrections in coastal regions: and implications for mean sea surface determination.” In *Coastal altimetry*, edited by S Vignudelli, A.G Kostianoy, P. Cipollini and J Benveniste Berlin Springer
- AVISO (2010) Coastal and hydrology altimetry product (PISTACH) handbook. 58
- Bernhoff H, Sjøstødt E, Leijon M (2006) Wave energy resources in sheltered sea areas: a case study of the Baltic Sea. *Renew Energy* 31: 2164–2170
- Bulhoes E, Fernandez GB (2011) “Analysis of Shallow Water Wave Propagation and Coastal Response in Embayed Beaches. Case Study in Cape Buzios, Rio de Janeiro, Brazil.” *Journal of Coastal Research*, Special Issue 64:2022–2026.

- Cipollini P, Benveniste J, Bouffard J, Emery W, L. Fenoglio Marc, Gommenginger C, Griffin D, Hoyer J, Kurapov A, Madsen K, Mercier F, Miller L, Pascual A, Ravichandran M, Shillington F, Snaith H, Strub PT, Vandemark D, Vignudelli S, Wilkin J, Woodworth P, and Garay JZ (2010) "The role of altimetry in coastal observing system." Proceeding of OceanObs '09 : Sustained ocean observations and information of society, Venice, Italy, 21–25 September
- Cipollini P, Coelho H, Fernandes J, Gomez-Enri J, Gommenginger C, Martin-Puig C, Vignudelli S, Woodworth P, and Benveniste J (2008) "Developing radar altimetry in the oceanic coastal zone: the COASTALT project." IGARSS 2008, Boston, USA, 6–11 July
- Cipollini P, Gommenginger C, Coelho H, Fernandes J, Gomez-Enri J, Martin-Puig C, Vignudelli S, Woodworth P, Dinardo S, Benveniste J (2009) Progress in coastal altimetry: the experience of the COASTALT Project. Geophys Res Abstr 11:EGU2009–EG12862 EGU General Assembly 2009
- Deng X, Featherstone WE (2006) A coastal retracking system for satellite radar altimeter waveforms: application to ERS-2 around Australia. J Geophys Res 111. <https://doi.org/10.1029/2005JC003039>
- Dinardo S, Lucas B, Gommenginger C, and Martin-Puig C (2013) Detailed processing model of the Sentinel-3 SRAL SAR altimeter sea waveform retracker-v2.3.0. European Space Agency Contract 20698/07/I-LG
- Fernandes J, Bastos L, and Antunes M (2003) "Coastal satellite altimetry-methods for data recovery and validation." 3rd meeting of the international gravity and geoid commission (GG2002)
- Gan J, Li H, Curchitser EN, Haidvogel DB (2006) Modeling South China Sea circulations: response to seasonal forcing regimes. J Geophys Res 111(C06034). <https://doi.org/10.1029/2005JC003298>
- Godijn Murphy LG, Miguez BM, McIlvenny J, Gleizon P (2015) Wave energy resource assessment with AltiKa satellite altimetry: a case study at a wave energy site. Geophys Res Lett 42:5452–5459. <https://doi.org/10.1002/2015GL064490>
- Gommenginger C, Thibaut P, Fenoglio-Marc L, Quartly G, Xiaoli Deng, Gomez-Enri J, Challenor P, and Gao Y (2011) "Retracking altimeter waveforms near the coasts. A review of retracking methods and some applications to coastal waveforms." In Coastal altimetry, edited by S. Vignudelli, A.G. Kostianoy, P. Cipollini and J Benveniste Berlin Springer
- Gommenginger CP, Srokosz MA, Challenor PG (2003) Measuring ocean wave period with satellite altimetry: a simple empirical model. Geophys Res Lett 30(22):2150
- Govindan R, Kumar R, Basu S, Sarkar A (2011) Altimeter-derived ocean wave period using generic algorithm. IEEE Geosci Remote Sens Lett 8:354–358
- Hwang PA, Teague WJ, Jacobs GA, Wang DW (1998) A statistical comparison of wind speed, wave height and wave period derived from satellite altimeters and ocean buoys in the Gulf of Mexico region. J Geophys Res 103(C5):10,451–10,468
- Idris NH (2014) "Development of new retracking methods for mapping sea levels over the shelf areas from satellite altimetry data." Doctor of Philosophy, School of Engineering The University of Newcastle, Australia
- Idris NH, Deng X (2012) The retracking technique on multi-peak and quasi-specular waveforms for Jason-1 and Jason-2 missions near the coast. Mar Geod 35:1–21. <https://doi.org/10.1080/01490419.2012.718679>
- Idris N, Deng X, Andersen OA (2014) The importance of coastal altimetry retracking and detiding: a case study around the Great Barrier Reef, Australia. Int J Remote Sens 35(5):1729–1740. <https://doi.org/10.1080/01431161.2014.882032>
- Idris N, Deng X, Din AHM, Idris N, H (2017) CAWRES: A waveform retracking fuzzy expert system for optimizing coastal sea levels from Jason-1 and Jason-2 satellite altimetry data. Remote Sens 9(603):1–22. <https://doi.org/10.3390/rs9060603>
- Justin TT, Dwarakish GS (2015) "Numerical wave modelling-A Review." Aquatic Procedia 4:443–448.
- Kofoed JP, Pecher A, Margheritini L, Antonishen M, Bittencourt C, Holmes B et al. (2013) "A methodology for equitable performance assessment and presentation of wave energy converters based on sea trials." Renew Energy 52:99–110
- Kramer M, Marquis L, and Frigaard P (2011) "Performance evaluation of the waviestar prototype." EWTEC 2011, Southampton, UK, 6 September 2011
- Kshatriya J, Sarkar A, Kumar R (2005) Determination of ocean wave period from altimeter data using wave-age concept. Mar Geod 28: 71–79
- Kumar VS, Anoop TR (2015) Wave energy resource assessment for the Indian shelf seas. Renew Energy 76:212–219
- Kuo HT, Shum CK, Chao Y, Emery WJ, Fok H, Lee H, Kuo C, and Yi Y (2011) "Radar altimetry waveform retracking applied to coastal ocean." 5th Coastal Altimetry Workshop, San Diego, USA, 16–18 October
- Madsen EF, Soerensen HC, and Parmeggiani S (2012) "Wave Dragon: multi-MW ocean energy power plant." International Conference on Ocean Energy, Dublin, Ireland
- Margheritini L, Vicinanza D, and Kofoed JP (2007) "Hydraulic characteristics of seawave slot-cone generator pilot plant at Kvitsøy (Norway)." Proceedings of the 7th European Wave and Tidal Energy Conference
- Mirzaei A, Tangang F, Juneng L (2014) Wave energy potential along the east coast of Peninsular Malaysia. Energy 68:722–734
- Muzathik AM, Wan Nik WB, Ibrahim MZ, Samo KB (2010) Wave energy potential of Peninsular Malaysia. ARPN J Eng Appl Sci 5(7):11–23
- Muzathik AM, Wan Nik WB, Samo KB, Ibrahim MZ (2011) Ocean wave measurement and wave climate prediction of Peninsular Malaysia. J Phys Sci 22(1):77–92
- Passaro M, Cipollini P, Vignudelli S, Quartly G, Snaith H (2014) ALES: a multi-mission adaptive subwaveform retracker for coastal and open ocean altimetry. Remote Sens Environ 145:173–189. <https://doi.org/10.1016/j.rse.2014.02.008>
- Pontes MT, Bruck M, and Lehner S. 2009. "Assessing the wave energy resources using remote sensed data." Proceedings of the 8th European Wave and Tidal Energy Conference, Uppsala, Sweden
- Power, Pelamis Wave (2017) Pelamis Wave Power Brochure. United Kingdom
- Raney RK (1998) The Delay/Doppler radar altimeter. IEEE Geosci Remote Sens 36(5):1578–1588
- Raynal M, Labroue S, Moreau T, Boy F, and Picot N (2018) "From conventional to Delay Doppler altimetry: a demonstration of continuity and improvements with the Cryosat-2 mission." *Advances in Space Research*:1–12. <https://doi.org/10.1016/j.asr.2018.01.006>
- Ren JL, Luo YY, Chen JJ, Zhang XM, Zhong YJ (2009) Research on wave power application by the information system for ocean wave resources evaluation. Renew Energ Resour 3(028)
- Sepulveda HH, Queffeuilou P, Arduin F (2015) Assessment of SARAL/AltiKa wave height measurements relative to buoy, Jason-2 and Cryosat-2 data. Mar Geod 38(Issue sup1):449–465
- Spataru C, Kok YC, Barrett M (2014) Physical energy storage employed worldwide. Energy Procedia 62:452–461
- Stopa JE, Filipot JF, Li N, Cheung KF, Chen YL, Vega L (2013) Wave energy resources along the Hawaiian island chain. Renew Energy 55:305–321
- Thibaut P, Aublanc J, Moreau T, Boy F, and Picot N (2014) "Delay/Doppler waveform processing in coastal zones." 8th Coastal Altimetry Workshop, Konstanz, Germany
- Valladeau G, Thibaut P, Picard B, Poisson JC, Tran N, Picot N, Guillot A (2015) Using SARAL/AltiKa to improve Ka-band altimeter measurements for coastal zones, hydrology and ice: the PEACHI

- prototype. *Mar Geod* 38(Sup1):124–142. <https://doi.org/10.1080/01490419.2015.1020176>
- Verron J (2013) “SARAL/AltiKa: a Ka band altimetric mission.” AVISO User Newsletter: Special SARAL/AltiKa Issue, 1
- Vignudelli S, Kostianoy AG, Cipollini P, Benveniste J (2011) Coastal altimetry. Springer, Berlin
- Wan Nik WB, Ibrahim MZ, Samo KB (2010) Wave energy potential of Peninsular Malaysia. *ARPN J Appl Sci* 5:11–23
- Wan Y, Zhang J, Meng J, Wang J (2015) A wave energy resources assessment in the China’s seas based on multi-satellite merged radar altimeter data. *Acta Oceanol Sin* 34(3):115–124
- Yaakob O, Hashim FE, Mohd Omar K, Md Din AH, Kho KK (2016) Satellite-based wave data and wave energy resource assessment for South China Sea. *Renew Energy* 88:359–371
- Zheng CW, Li X (2011) Wave energy resources assessment in the China Sea during the last 22 years by using WAVEWATCH-III wave model. *Periodical of Ocean Univ China (in Chinese)* 41(11):5–12
- Zheng CW, Pan J, Li JX (2013) Assessing the China Sea wind energy and wave energy resources from 1988 to 2009. *Ocean Eng* 65:39–48
- Zheng CW, Zheng Y, Chen H (2011) Research on wave energy resources in the northern South China Sea during recent 10 years using SWAN wave model. *Journal of Subtropical Resources and Environment (in Chinese)* 6(2):54–59
- Zheng CW, Li CY, Chen X, Pan J (2016) Numerical forecasting experiment of the wave energy resource in the China Sea. *Adv Meteorol* 2016:1–12
- Zubaidah I, Siti Zawiah MD, and Ramlee K (2006) “The fifth energy option for Malaysia.” *JURUTERA*:16–19